Supporting Information: Neptunium and Uranium Interactions with Environmentally and Industrially Relevant Iron Minerals

Luke T. Townsend, Kurt F. Smith, Ellen H. Winstanley, Katherine Morris, Olwen Stagg, J. Frederick W. Mosselmans, Francis R. Livens, Liam Abrahamsen-Mills, Dick Blackham and Samuel Shaw *

Np L_{III} edge XANES data.

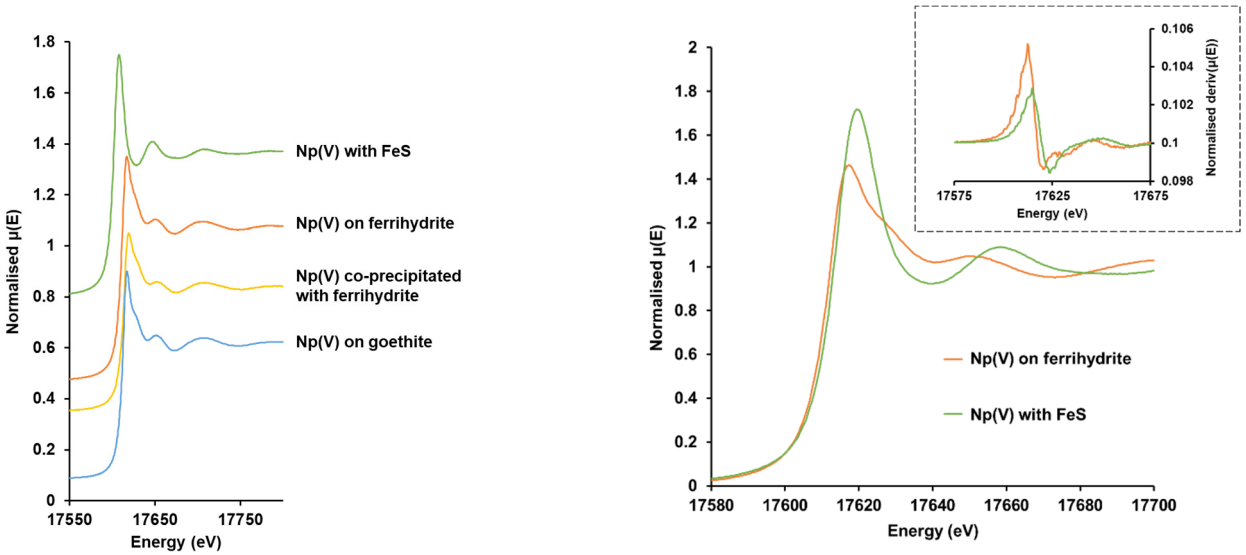

Figure S1. Np L_{III}-edge XANES spectra of the Np with iron mineral samples. Left: the uncalibrated XANES of each sample. Right: the calibrated XANES data for Np(V) on ferrihydrite and Np(V) with FeS with the derivative shown in the insert.

Detailed EXAFS Analysis & Discussion

This section aims to further expand on the discussion in the main manuscript regarding the possible EXAFS models for the Np(V)-neptunyl systems (Np(V) on ferrihydrite, Np(V) co-precipitated with ferrihydrite, and Np(V) on goethite). The analysis provided in Figures S2 & S3 and Tables S1 & S2 investigate how well the EXAFS data can be modelled through the gradual introduction of more complex fitting models.

Four different fitting models are shown below, labelled Models 1–4. Model 1 is the simple fit shown in the main manuscript whereby one O_{ax} shell and one O_{eq} shell are used to build the model. From here, Models 2–4 were built to test how the addition of various different shells (informed by the chemistry of the system and relevant literature) impacted the models. Each time, multiple fits were tested and only the best fits for each model was presented (for example, of the three Model 4 fits shown, two contain C shells and one does not). This was decided based upon which model produced the quantitative and qualitative best fit. Model 2 splits the O_{eq} shell into two O_{eq} shells at two different interatomic distances. Model 3 tests how the addition of a C shell impacts the fit. Model 4 tests how the addition of an Fe shell impacts the fit. Overall, all the models appear to be qualitatively similar, with small changes in the highlighted areas for added C and Fe shells (Figure S2). Any additional components to the models after the initial simple two shell fit (Model 1) do not drastically qualitatively improve the fit of the model to the data, however, the quantitative components of the fit (i.e., R-factor, number of variables used, Debye-Waller factors, and interatomic distances) are all changed significantly between models.

Following the discussion of the 4 fitting models for each system, an analysis of the impact of the introduction of multiple scattering pathways is provided (Figure S3, Table S2).

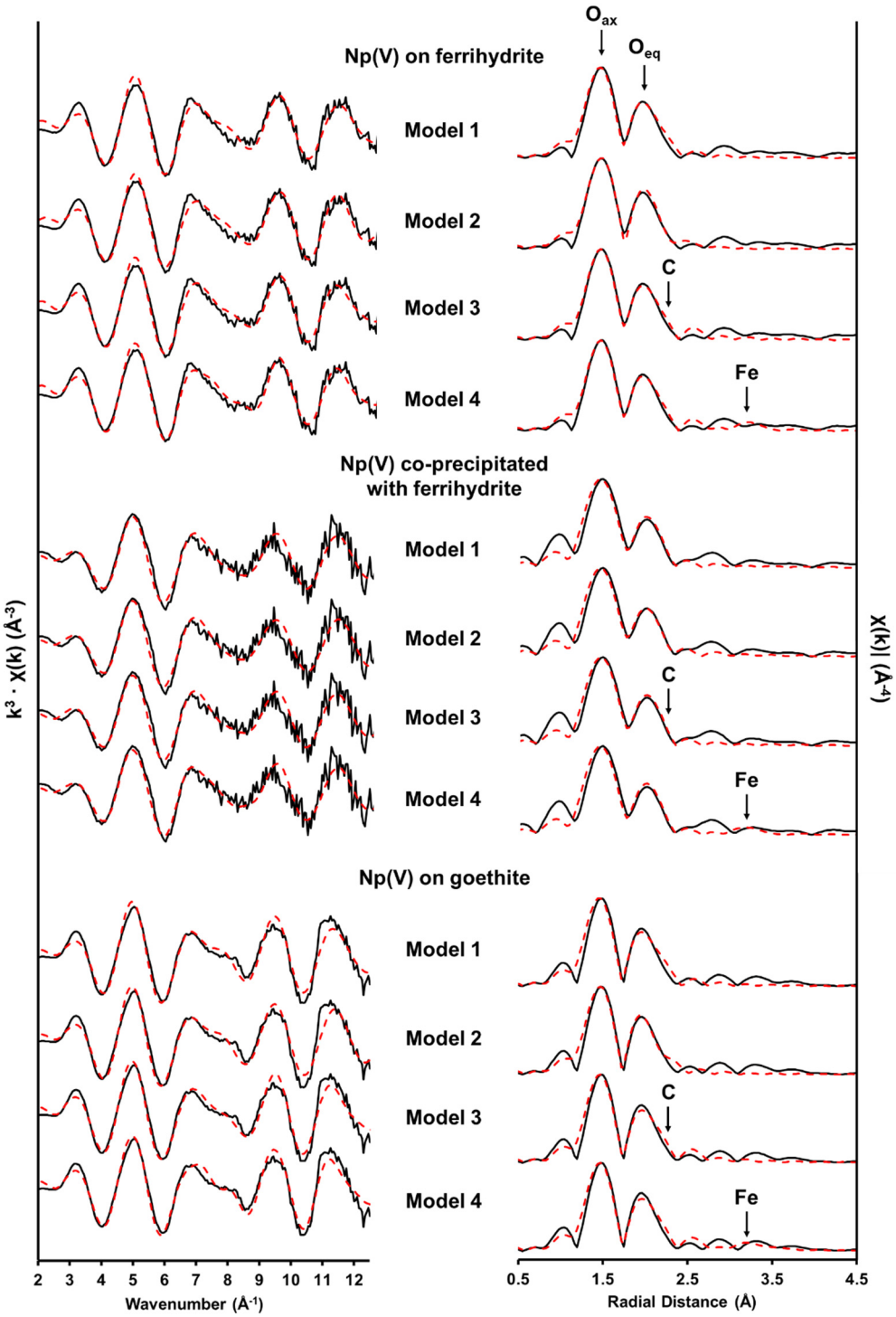

Figure S2. Alternate fit options for the Np L_{III}-edge EXAFS data from the Np(V) on ferrihydrite, Np(V) co-precipitated with ferrihydrite, and Np(V) on goethite systems. Model 1 is a simple two shell fit with O_{ax} and O_{eq} shells. Model 2 builds on Model 1 by splitting the O_{eq} shell. Model 3 contains in a C shell. Model 4 contains in a Fe shell. Further details on the fitting models are provided in Table S1.

Table S1. EXAFS fitting parameters for the different models (1–4) shown in Figure S2. All nomenclature used is identical to the main manuscript. * indicates parameters were linked.

		Model 1			Model 2			Model 3			Model 4		
	Path	**N**	**σ² (Å²)**	**R (Å)**	**N**	**σ² (Å²)**	**R (Å)**	**N**	**σ² (Å²)**	**R (Å)**	**N**	**σ² (Å²)**	**R (Å)**
Np(V) on ferrihydrite $S_0^2 = 0.9$ *k*-range = 3–13.5	O_{ax}	2	0.002(1)	1.86(1)	2	0.002(1)	1.87(2)	2	0.002(1)	1.87(1)	2	0.002(1)	1.87(1)
	$O_{eq}1$	5	0.008(2)	2.49(3)	2.5	0.002(2)	2.47(10)	5	0.008(2)	2.50(3)	5	0.008(2)	2.49(3)
	$O_{eq}2$				2	0.008(4)	2.61(5)						
	C							1	0.003(12)	2.83(10)	1	0.003(11)	2.82(9)
	Fe										1	0.011(98)	3.59(10)
		$E_0 = -2.2(21)$	R-factor = 0.0192		$E_0 = 0.1(31)$	R-factor = 0.0187		$E_0 = -1.1(23)$	R-factor = 0.0179		$E_0 = -1.2(21)$	R-factor = 0.0240	
		R-range = 1.25–2.7	Variables = 5 of 9.6		*R*-range = 1.25–2.7	Variables = 7 of 9.6		*R*-range = 1.25–2.9	Variables = 7 of 10.8		*R*-range = 1.25–3.5	Variables = 9 of 14.9	
Np(V) co-precipitated with ferrihydrite $S_0^2 = 0.9$ *k*-range = 3–12	O_{ax}	2	0.001(1)	1.86(1)	2	0.002(1)	1.87(2)	2	0.001(1)	1.86(2)	2	0.001(1)	1.85(1)
	$O_{eq}1$	5	0.009(2)	2.46(2)	3	0.005(5)*	2.47(10)	5	0.009(2)	2.46(4)	5	0.009(2)	2.46(2)
	$O_{eq}2$				2	0.005(5)*	2.61(5)						
	C							1	0.013(50)	2.83(30)			
	Fe										1	0.012(12)	3.52(9)
		$E_0 = -5.7(19)$	R-factor = 0.0168		$E_0 = -5.5(26)$	R-factor = 0.0200		$E_0 = -5.1(31)$	R-factor = 0.0254		$E_0 = -5.9(19)$	R-factor = 0.0368	
		R-range = 1.1–2.6	Variables = 5 of 8.4		*R*-range = 1.1–2.7	Variables = 6 of 9.1		*R*-range = 1.1–3	Variables = 7 of 10.7		*R*-range = 1.1–3.5	Variables = 9 of 14.2	
Np(V) on goethite $S_0^2 = 1.0$ *k*-range = 3–13.5	O_{ax}	2	0.001(1)	1.85(1)	2	0.001(1)	1.86(1)	2	0.001(1)	1.86(1)	2	0.001(1)	1.86(1)
	$O_{eq}1$	5	0.007(2)	2.49(3)	3	0.002(3)*	2.45(3)	5	0.006(2)	2.50(3)	5	0.007(2)	2.50(2)
	$O_{eq}2$				2	0.002(3)*	2.59(3)						
	C							1	0.002(10)	2.82(9)	1	0.001(9)	2.82(8)
	Fe										1	0.009(11)	3.68(9)
		$E_0 = -3.5(20)$	R-factor = 0.0248		$E_0 = -2.7(22)$	R-factor = 0.0234		$E_0 = -2.5(20)$	R-factor = 0.0212		$E_0 = -2.4(19)$	R-factor = 0.0285	
		R-range = 1.25–2.7	Variables = 5 of 9.6		*R*-range = 1.25–2.7	Variables = 6 of 9.6		*R*-range = 1.25–2.9	Variables = 7 of 10.8		*R*-range = 1.25–3.5	Variables = 9 of 14.9	

Np(V) on ferrihydrite

In this system, Models 1–3 provide generally good fits (R-factor <0.02). Model 4 has a slightly raised R-factor (0.024) which indicates, when compared to the other models, that this model is likely incorrect. The addition of the Fe shell in the Model 4 fit can be seen to cause significant misfit in the Fourier transform at ~3 Å (Figure S2). This shows that the addition of an Fe backscatterer to the model does not provide an adequate description of the system however, as discussed in the main manuscript, this does not exclude the possibility of the formation of an inner sphere complex forming, principally due to the difficulty of fitting such a shell with certainty [12,15,16,19,64]. Interestingly, Model 3 provides the best quantitative fit (R-factor = 0.0179) due to the addition of the C backscatterer however, chemically this model does not seem to be the most realistic for the system. Given the sample was prepared with atmospheric levels of carbonate present in solution, and given (as discussed in the main manuscript) that a carbonate enriched solution (10 mM bicarbonate in the Np(V)/goethite system) only gives rise to ~10% $Np(V)O_2(CO_3)^-$ as the sole Np(V)-carbonate species, the formation of this species seems unlikely. Whilst there is some evidence for crystalline iron (oxyhydr)oxides encouraging the formation of Np(V)-carbonates at the surface of the mineral [15], this study was performed on a more crystalline phase (eg. hematite) [15] and so it seems more likely that the addition of a soft backscatterer (in this case C) is resulting in overfitting of the data. Models 1 and 2 provide quantitatively similar fits (Model 1 R-factor = 0.0192; Model 2 R-factor = 0.0187) with the difference being a split O_{eq} coordination in Model 2. This model would suggest a possible inner sphere complexation as the splitting of the equatorial O ligands to two different interatomic distances is common for actinyl moieties adsorbing to iron (oxyhydr)oxides [36,71]. However, F-test results show that the marginal improvement of Model 2 over Model 1 is not statistically significant (F-test = 6.6%) and therefore the most reliable and robust model is Model 1.

Np(V) co-precipitated with ferrihydrite

Model 1 and 2 are the only models that provide a quantitatively good fit for this system, with the simple Model 1 providing the best fit for the data by a significant margin (Model 1 R-factor = 0.0168; Model 2 R-factor = 0.0200). Whilst Model 2 provides a statistically acceptable fit, the overall R-factor is worse than Model 1, therefore the splitting of the O_{eq} shell difficult to justify. However, as with the previous system, this does provide some further evidence that an inner sphere sorption complex may be forming at the surface of the ferrihydrite. Model 3 has a slightly raised R-factor (0.0254) compared to Models 1 and 2 and given the previous discussions on the likelihood of Np(V)-carbonate species formation, is unlikely to be an adequate model for the speciation of Np(V) in this system. Model 4 is quantitatively poor (R-factor = 0.0368), with the addition of an Fe backscatterer providing no benefit to model. Here, the Fe backscatterer is seemingly attempting to fit the background noise and therefore it is not possible to discern whether an Fe is present in this system. As with the Np(V) on ferrihydrite system, the most robust fitting model is the simple two shell fit (Model 1).

Np(V) on goethite

The Np(V) on goethite system proved the most problematic when attempting to produce a quantitatively good fit, with all fits marginally exceeding the boundary for a good fit (R-factors = 0.0212–0.0285). Interestingly, the best fit for this system was Model 3 (R-factor = 0.0212) suggesting a carbonate ligand may be present. F-test analysis for the addition of the carbonate shell to Model 1 to produce Model 3 suggests that the improvement, whilst not statistically significant (75.2%), is measurable. Additionally, as the goethite system has 10 mM bicarbonate in solution, PHREEQC modelling suggests that there may be some carbonate complexation to $Np(V)O_2^+$ in solution (as discussed in the main

manuscript). Furthermore, previously discussed work has highlighted the possibility for crystalline iron oxides to produce Np(V)-carbonate species at mineral surfaces [15]. As goethite is a crystalline phase, Model 3 may be a valid species model for this system. Model 4 is a significantly quantitatively worse fit than Models 1–3 and also shows misfit in the Fourier transform at ~3.2 Å where the Fe backscatterer seemingly manifests. As with the previously discussed co-precipitation system, the addition of an Fe backscatterer seemingly fits the background noise and so is not a valid addition to the model. Whilst the splitting of the O_{eq} shell to produce Model 2 from Model 1 does produce a quantitative improvement, F-test analysis shows the lowering of the R-factor (from 0.0248 to 0.0234) to be statistically insignificant (F-test = 45.4%). This means Models 1 and 3 are the most likely candidates for describing the Np(V) speciation in this system. Whilst Np(V)-carbonate species may form more readily at the surface of a mineral phase like goethite, the lack of significant statistical improvement upon the addition of the C backscatterer means that Model 1 is the most robust and defendable fit. However, the possible presence of a Np(V)-carbonate species (likely $Np(V)O_2(CO_3)^-$) at the surface of goethite cannot be fully disregarded.

Multiple Scattering Pathways

As a means to demonstrate the effect of the addition of multiple scattering pathways on these models, the Np(V) on goethite system was chosen. Here, Model 1 was compared to Model 1A which contains the three most prevalent O_{ax} multiple scattering pathways; the rattle (MS1), the non-forward through absorber (MS2), and the forward through absorber (MS3). Upon the addition of these multiple scattering pathways, the fit is significantly worsened, both qualitatively and quantitatively. In the Fourier transform, significant misfit can be observed in Figure S3 at ~3.2 Å, and a pronounced shift in the O_{ax} component of the fit. Quantitatively, the fit is considerably worse with the R-factor increasing from 0.0284 (Model 1) to 0.0594 (Model 1A) indicating the fit is incorrect. This highlights the difficulties associated with analysing EXAFS data of transuranic elements and is likely attributed to the non-linear neptunyl moiety (bond angle varying from 171° to 177°) [58,59]. A consequence of a non-linear neptunyl moiety is that the data range used in this study may be insufficient for observing the effects of the O_{ax} multiple scatterers. As can be seen in Figure S4, the O_{ax} multiple scattering pathways all have maximum amplitudes at approximately 18–20 $Å^{-1}$ in *k*-space and so a significantly larger data range may be needed to accurately fit these pathways to the data.

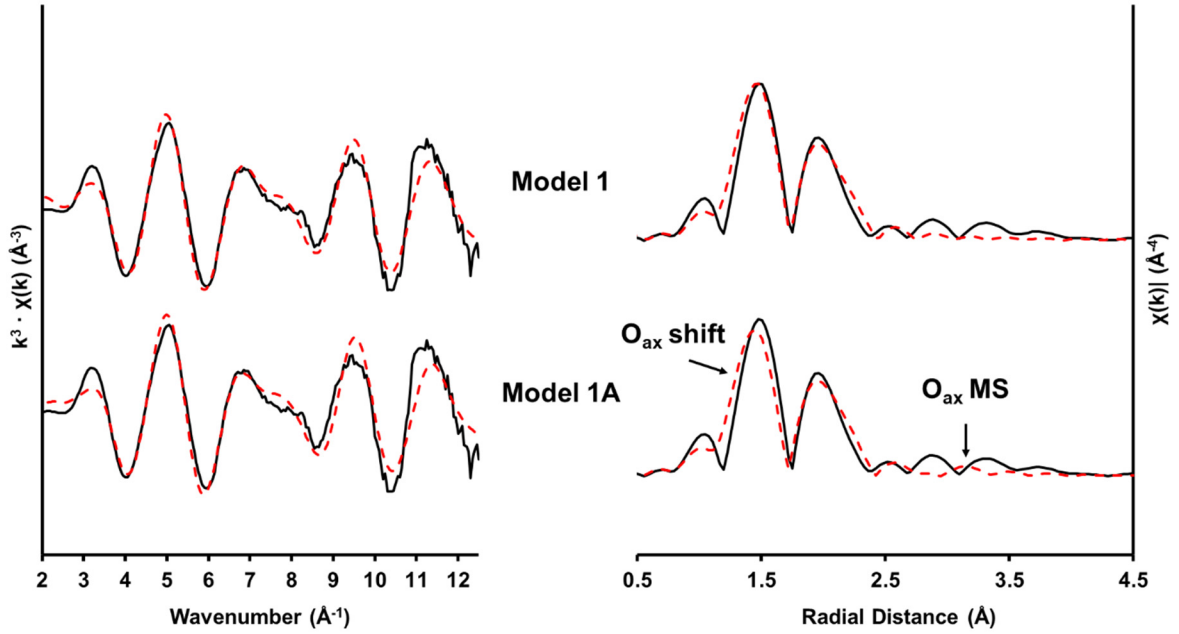

Figure S3. Np L_{III}-edge EXAFS spectra from the Np(V) in goethite system with different fitting models to accommodate multiple scattering pathways. Model 1 is the simple fit described in detail earlier. Model 1A adds in the O_{ax} multiple scattering pathways MS1-3 (rattle, non-forward through absorber, and forward through absorber).

Table S2. EXAFS fitting parameters for the Np(V) on goethite models shown in Figure S3, demonstrating the effect of adding multiple scattering pathways to the fit.

	Model 1			**Model 1A (Additional O_{ax} Multiple Scatterers)**		
Path	**N**	**σ^2 (Å^2)**	**R (Å)**	**N**	**σ^2 (Å^2)**	**R (Å)**
O_{ax}	2	0.001(1)	1.85(1)	2	0.001(1)	1.84(1)
$O_{eq}1$	5	0.007(2)	2.49(3)	5	0.006(2)	2.48(2)
O_{ax} MS 1				2	0.001(1)	3.82(4)
O_{ax} MS 2				2	0.001(1)	3.69(2)
O_{ax} MS 3				2	0.001(1)	3.69(2)
	E_0 = –3.5(20)	R-factor = 0.0248		E_0 = –4.9(20)	R-factor = 0.0594	
	R-range = 1.25–2.7	Variables = 5 of 9.6		*R*-range = 1.25–3.6	Variables = 5 of 15.5	

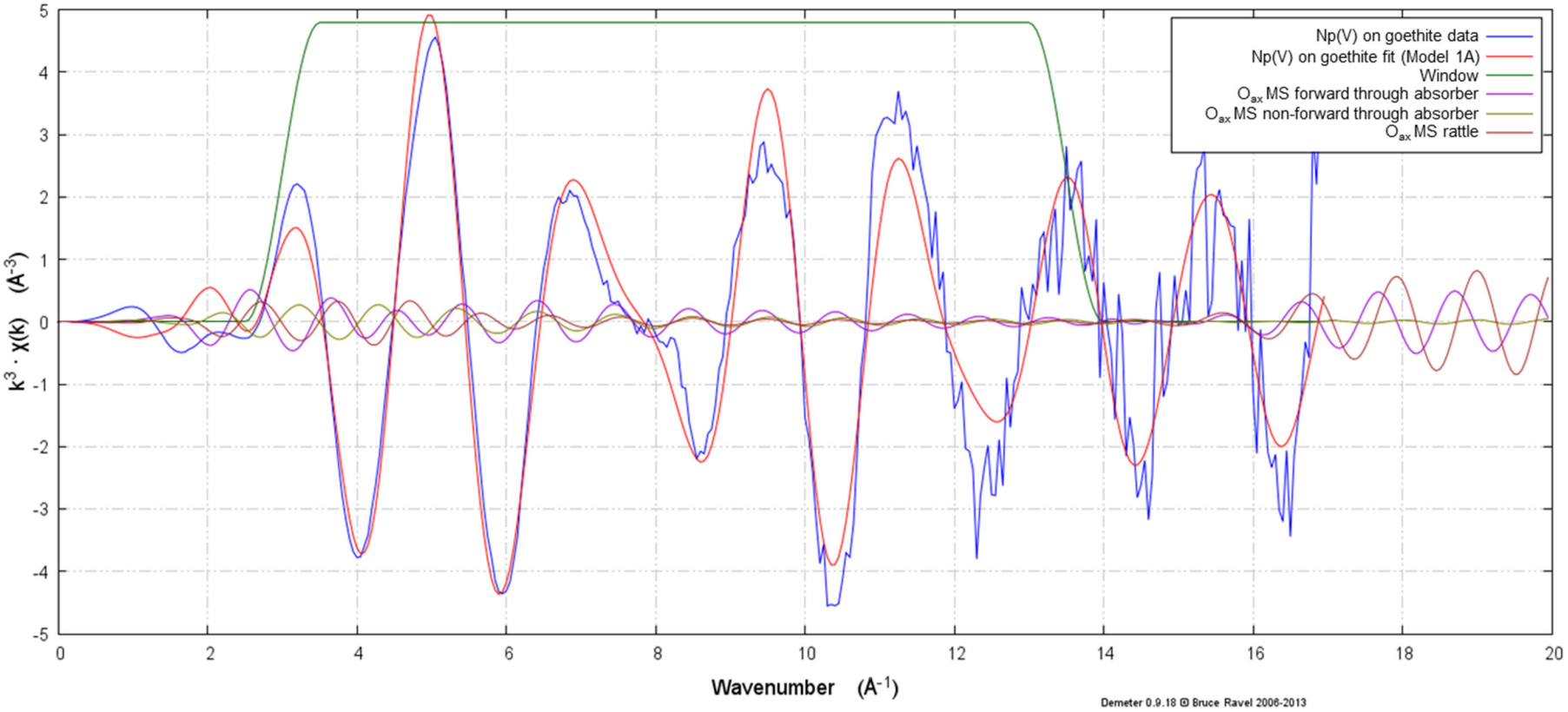

Figure S4. EXAFS *k*-space plot of the Np(V) on goethite sample showing the data, the Model 1A fit, and the O_{ax} multiple scattering pathways (forward through absorber, non-forward through absorber, and rattle).

U LIII edge XANES data

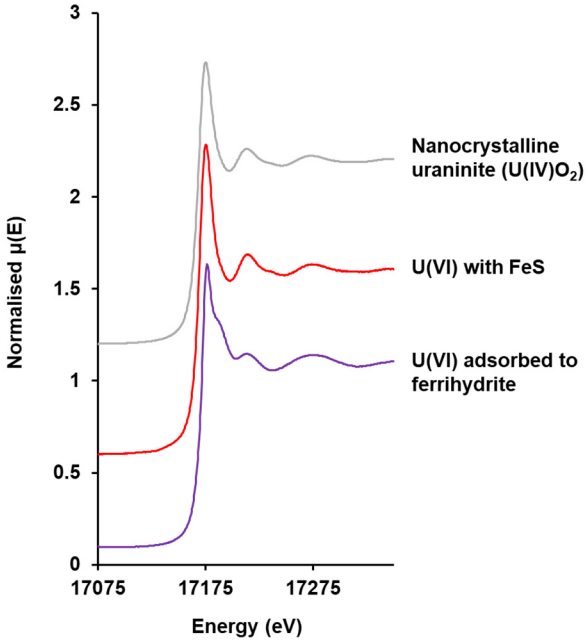

Figure S5. U LIII-edge XANES spectra of U(VI) with FeS and two end member species (U(VI) adsorbed to ferrihydrite and nanocrystalline uraninite ($U(IV)O_2$)) standards taken from previous work [26,42].

References

12. Bots, P.; Shaw, S.; Law, G.T.W.; Marshall, T.A.; Mosselmans, J.F.W.; Morris, K. Controls on the Fate and Speciation of Np(V) During Iron (Oxyhydr)Oxide Crystallization. *Environ. Sci. Technol.* **2016**, *50*, 3382–3390.

15. Arai, Y.; Moran, P.; Honeyman, B.; Davis, J. In Situ Spectroscopic Evidence for Neptunium (V)-Carbonate Inner-Sphere and Outer-Sphere Ternary Surface Complexes on Hematite Surfaces. *Environ. Sci. Technol.* **2007**, *41*, 3940–3944.

16. Combes, J.M.; Chisholm-Brause, C.J.; Brown, G.E.; Parks, G.A.; Conradson, S.D.; Eller, P.G.; Triay, I.R.; Hobart, D.E.; Miejer, A. Exafs Spectroscopic Study of Neptunium(V) Sorption at the A-Feooh/Water Interface. *Environ. Sci. Technol.* **1992**, *26*, 376–382.

19. Müller, K.; Gröschel, A.; Rossberg, A.; Bok, F.; Franzen, C.; Brendler, V.; Foerstendorf, H. In Situ Spectroscopic Identification of Neptunium (V) Inner-Sphere Complexes on the Hematite–Water Interface. *Environ. Sci. Technol.* **2015**, *49*, 2560–2567.

26. Townsend, L.T.; Shaw, S.; Ofili, N.E.R.; Kaltsoyannis, N.; Walton, A.S.; Mosselmans, J.F.W.; Neill, T.S.; Lloyd, J.R.; Heath, S.; Hibberd, R., et al. Formation of a U(Vi)–Persulfide Complex During Environmentally Relevant Sulfidation of Iron (Oxyhydr)Oxides. *Environ. Sci. Technol.* **2020**, *54*, 129–136.

36. Waite, T.D.; Davis, J.A.; Payne, T.E.; Waychunas, G.A.; Xu, N. Uranium(Vi) Adsorption to Ferrihydrite: Application of a Surface Complexation Model. *Geochim. Cosmochim. Acta* **1994**, *58*, 5465–5478.

42. Townsend, L.T.; Morris, K.; Harrison, R.; Schacherl, B.; Vitova, T.; Kovarik, L.; Pearce, C.I.; Mosselmans, J.F.W.; Shaw, S. Sulfidation of Magnetite with Incorporated Uranium. *Chemosphere* **2021**, *276*, 130117.

58. Elo, O.; Müller, K.; Ikeda-Ohno, A.; Bok, F.; Scheinost, A.C.; Hölttä, P.; Huittinen, N. Batch Sorption and Spectroscopic Speciation Studies of Neptunium Uptake by Montmorillonite and Corundum. *Geochim. Cosmochim. Acta* **2017**, *198*, 168–181.
59. Forbes, T.Z.; Burns, P.C.; Skanthakumar, S.; Soderholm, L. Synthesis, Structure, and Magnetism of Np2o5. *Journal of the American Chemical Society* **2007**, *129*, 2760–2761.
64. Sherman, D.M.; Peacock, C.L.; Hubbard, C.G. Surface Complexation of U(Vi) on Goethite (A-Feooh). *Geochim. Cosmochim. Acta* **2008**, *72*, 298–310.
71. Catalano, J.G.; Brown, G.E. Uranyl Adsorption onto Montmorillonite: Evaluation of Binding Sites and Carbonate Complexation. *Geochim. Cosmochim. Acta* **2005**, *69*, 2995–3005.